

# A245 : Optical Frequency Doubling

*A lab report written by*

Group P20: Mrunmoy Jena and Ajay Shanmuga Sakthivasan

**Supervisor: Thilina Muthu-Arachchige**

Universität Bonn

May 23, 2022

# Contents

<b>Abstract</b>	<b>1</b>
<b>1 Introduction</b>	<b>2</b>
<b>2 Experiment and Analysis of Results</b>	<b>3</b>
2.1 Power measurements of the diode laser . . . . .	3
2.1.1 Calibration of removable attenuator . . . . .	4
2.1.2 Calculation of unattenuated power values above $19\ \mu\text{W}$ . . . . .	5
2.1.3 Study of dependence of fundamental output power on the injection current . . . . .	6
2.1.4 Calculation of laser output characteristics . . . . .	7
2.1.5 Calibration of variable attenuator . . . . .	7
<b>A Appendix</b>	<b>10</b>

# Abstract

xyz

# Introduction

# Experiment and Analysis of Results

This section discusses the experimental setup and procedure, along with the calculation of the necessary quantities and their error analysis.

To begin with, a class 3B external cavity diode laser (TuiOptics, DL100) emitting light of wavelength 987 nm is used for the experiment. A shutter mounted onto the laser controls the beam and a pair of anamorphic prisms is used to modify the elliptical beam profile to a more circular shape. The laser, shutter and prism pairs were all fixed on a laser table beforehand. For each part of the experiment, other instruments and optical elements were added onto this setup.

## 2.1 Power measurements of the diode laser

The first part of the experiment is aimed at familiarizing oneself with the dependence of the fundamental output power of the laser with the injection current and to extract various important parameters characterizing the laser such as the threshold current, differential slope efficiency and the differential quantum efficiency.

In order to perform this experiment, a power meter was mounted on table in such a manner that it remains at the same height as that of laser beam as well as aligned with the beam (i.e. the face of the power meter is perpendicular to the beam axis). This adjustment was first performed by using an IR (infrared) detection card in order to ensure that the entire beam went into the power meter. Then the power meter is switched on, and the wavelength to be measured by it is set to 987 nm. Subsequently, finer adjustment is performed by moving the power meter to a position where it gives the maximum power reading. The power meter is then screwed tight at this position.

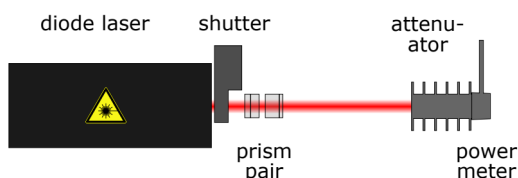


**Figure 2.1:** Set up to measure variation of laser output power with injection current [1]

The set up for this experiment (along with attenuator attached) is shown in Figure 2.1. With this setup in place, the injection current is increased from 0 to 280 mA in increments of 5 mA, and the corresponding values of output power are noted. Since the power meter sensor becomes non-linear for powers above 20 mW, it becomes necessary to use an attenuator. For our measurements, we took measurements both with and without attenuator in the unattenuated power range from  $28.2 \mu\text{W}$  to  $19000 \mu\text{W}$  (19 mW). Both the unattenuated and attenuated power values are necessary to be recorded over at least some data points in order to perform the calibration and extract a calibration factor from it. Beyond this range, the power is only measured with the attenuator attached onto the power meter, due to the aforementioned reason of non-linearity of the sensor. The attenuator for the experiment is a '1000:1' attenuator (meaning that

ideally it would reduce the unattenuated power by a factor of 1000). The recorded data can be found in A.1. The values measured without attenuator are listed under the column ‘ $P_{unatt}$ ’ and the measured power values with attenuator are under the column ‘ $P_{att}$ ’. From now on, all errors stated in the tables should be assumed to be instrumental errors (least count of the measuring instrument), unless otherwise stated.

### 2.1.1 Calibration of removable attenuator

In order to find the calibration factor, the data for the attenuated power vs. unattenuated power is plotted and a linear fit is applied to this dataset. To carry out the curve fitting procedure using the data points and some initial guess parameters, we used the function `curve_fit()` from the `scipy.optimize` module for *Python*. The data points (along with x-y error bars) and the linear fit modelled onto them is shown in Figure 2.2.

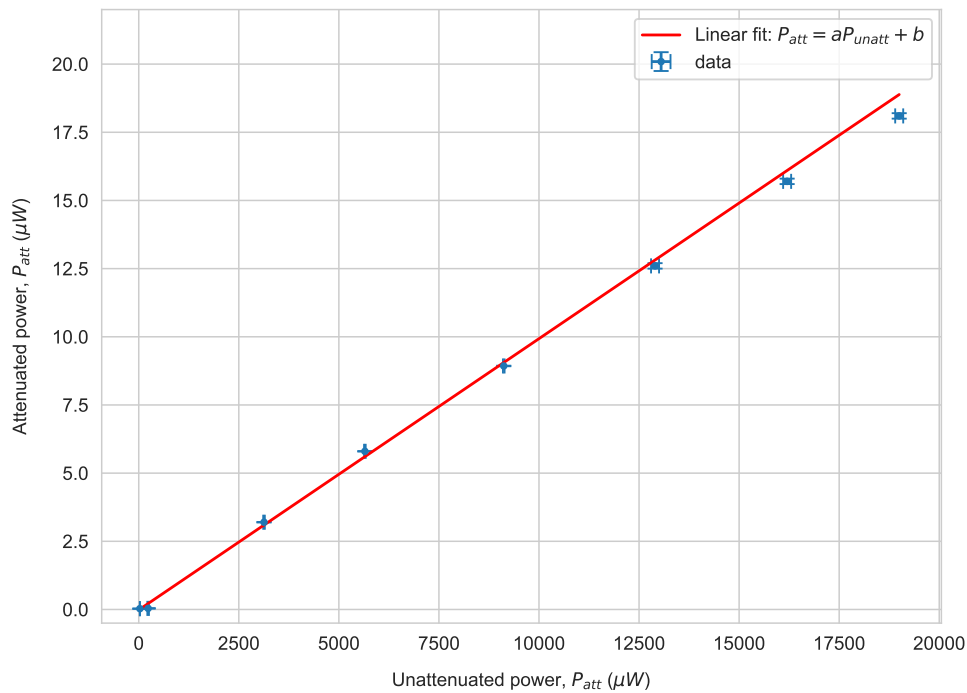


**Figure 2.2:** Calibration plot of attenuated output power vs unattenuated power

The linear fit chosen is of the form:

$$P_{att} = aP_{unatt} + b \quad (2.1)$$

The choice of the initial guess parameters is taken as  $a = 0.001$  (since as already mentioned before, attenuated power is around 1/1000 of the unattenuated power, due to use of ‘1000:1’ attenuator) and  $b = 0$  (y intercept expected to be a very small value, by visually extrapolating the data points). Indeed, after running the curve fitting procedure, we get fit parameters close to our initial guess:  $a = 0.000994 \pm$

$1.25 \times 10^{-6}$  and  $b = -0.016 \pm 0.006$ , giving:

$$P_{att} = (0.000994 \pm 1.25 \times 10^{-6})P_{unatt} + (-0.016 \pm 0.006)$$

Now we use the commonly applied reduced  $\chi^2$  test, to find the goodness of fit for this linear model:

$$\chi^2 = \sum_i \left[ \frac{y_i(x_i) - f_i(x_i; p)}{\sigma_i} \right]^2 \quad (2.2)$$

where  $y_i(x_i)$  are the recorded y values (attenuated power in this case),  $f_i(x_i; p)$  is are y values from the fitting function with  $p$  parameters (in this case the linear fit function with parameters  $a$  and  $b$ ).

Surprisingly, we get an extremely large reduced  $\chi^2$  value of 174.69. Naively, one would conclude that since  $\chi^2 \gg 1$ , the model is a 'bad fit'. However, on looking more carefully at the data points, we make two observations:

- We find that the error in the first five data points (corresponding to current ( $I$ ) values lying in the range of 50 to 70 mA) is an order of magnitude smaller than for the remaining data points. Given that the order  $\mathcal{O}(y_i(x_i) - f_i(x_i; p))$  remains the same (more or less), the  $\chi^2$  is sensitive to the order of the squares of the y-errors  $\mathcal{O}(\chi^2) \sim \mathcal{O}(1/\sigma_i^2)$ . As such, the contribution from the very small errors of the first five data values would be around 100 times compared to that from the remaining y values.
- Moreover, we only have a small number of data points ( $N = 8$ ), which we are trying to fit with two parameters ( $p = 2$ ), this restricts the degrees of freedom to only 6 ( $df = N - p$ ). Again this leads to a large reduced  $\chi^2$  value.

The combination of both these factors shows that in the case of small data sets, the error on the data points largely affects the reduced  $\chi^2$  value. Indeed, this is confirmed in a paper by Andrae et.al. [2]. However, here, since we are concerned with only extracting the calibration factor, we just want to check how well the linear regression line approximates the actual data values. For this we calculate the  $R^2$  (coefficient of determination):

$$R^2 = 1 - \frac{\sum_i (y_i - f_i(x_i; p))^2}{\sum_i (y_i - \bar{y})^2} \quad (2.3)$$

where  $\bar{y}$  is the mean of all the recorded data values

The  $R^2$  value indeed comes out to be very close to 1 ( $R^2 = 0.997$ ), meaning that our linear model explains 99.7% of all the variation of the y value (attenuated power) around its mean.

### 2.1.2 Calculation of unattenuated power values above 19 $\mu$ W

We recall that after the unattenuated power reached a value of 19  $\mu$ W, only attenuated power values were recorded. Therefore, in order to find the dependence of unattenuated power with the injection current, we need to use to calculate unattenuated power values above 19  $\mu$ W first, by applying the calibration factor to the attenuated power values. From Eq. 2.1 we get:

$$P_{unatt} = \frac{P_{att} - b}{a} \quad (2.4)$$

In addition to this, the errors on each of these calculated values will no longer be instrumental, but will be calculated from error propagation:

$$\Delta P_{unatt} = \sqrt{\left(\frac{\Delta P_{att}}{a}\right)^2 + \left(\frac{\Delta b}{a}\right)^2 + \left(\frac{\Delta a(P_{att} - b)}{a^2}\right)^2} \quad (2.5)$$

These calculated unattenuated power values and their errors are also included in Table A.1.

### 2.1.3 Study of dependence of fundamental output power on the injection current

Once all the unattenuated power values are obtained, the fundamental unattenuated power vs injection current is plotted. This plot is shown in Figure 2.3.

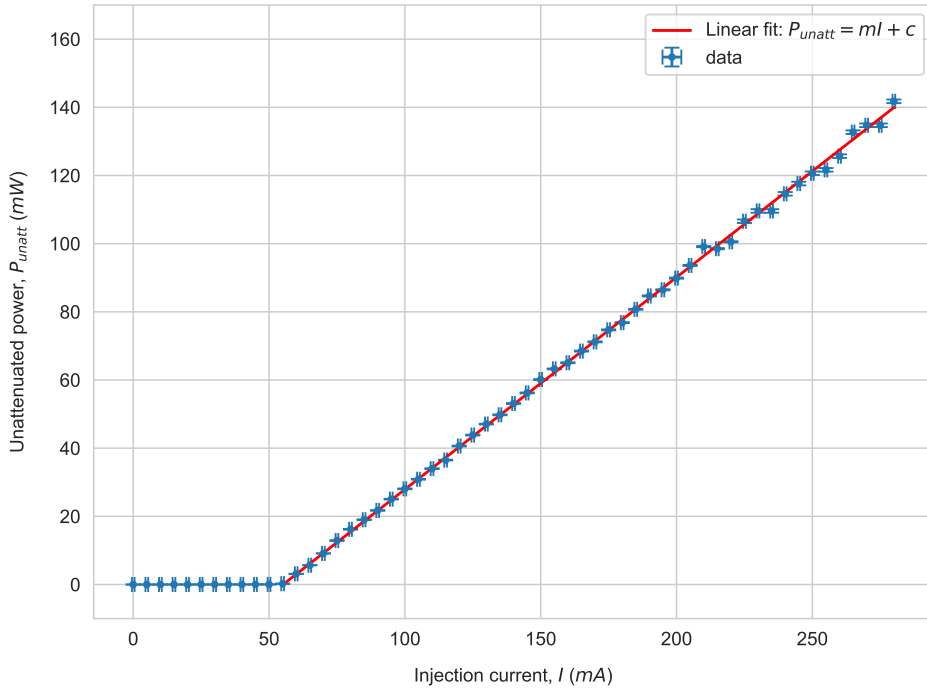


**Figure 2.3:** Plot of unattenuated output power vs injection current

One finds that the unattenuated power remains close to zero upto a certain value of the injection current (around 50 mA) and after this value, the fundamental power starts increasing linearly with the injection current. As such, for this linear region, we choose a linear fit of the form:

$$P_{unatt} = mI + c \quad (2.6)$$

After visually guessing the slope and the y intercept, we take initial parameters for curve fitting as  $m = 30/40 = 0.75$  and  $c = -30$ . The least square curve fitting procedure gives the best linear fit



as:

$$P_{unatt} = (0.62234 \pm 0.00027)I + (-34.329 \pm 0.022) \quad (2.7)$$

The  $R^2$  value for this fit is found to be 0.9993, indicating a linear model that explains the variability in y values quite well. Again, the  $\chi^2$  goodness of fit test isn't used here because of the complications mentioned in Section 2.1.1.

#### 2.1.4 Calculation of laser output characteristics

- **Threshold current:** The particular value of injection current, at which the output unattenuated power starts increasing from zero is called the threshold current and is given by:

$$I_0 = -\frac{c}{m} \quad (2.8)$$

while its error is found to be:

$$\Delta I_0 = \sqrt{\left(\frac{\Delta c}{m}\right)^2 + \left(\frac{c\Delta m}{m^2}\right)^2} \quad (2.9)$$

This gives a threshold current value of  $I_0 = 55.161 \pm 0.039$  mA

- **Differential slope efficiency:** The differential slope efficiency, in the case of this linear fit is simply the slope of the straight line:

$$\frac{\partial P}{\partial I} = \frac{P}{I} = m \quad (2.10)$$

with its error given as:

$$\Delta\left(\frac{\partial P}{\partial I}\right) = \Delta m \quad (2.11)$$

The result is then  $\frac{\partial P}{\partial I} = -34.329 \pm 0.022$  W/A

- **Quantum efficiency:** The quantum efficiency is given by the ratio of the number of photons that are emitted ( $N_\gamma$ ) to the number of injected electrons ( $N_e$ ). This is then given as:

$$\eta = \frac{N_\gamma}{N_e} = \frac{e}{h\nu} \frac{\partial P}{\partial I} \quad (2.12)$$

with error:

$$\Delta\eta = \frac{N_\gamma}{N_e} = \left(\frac{e}{h\nu}\right) \Delta\left(\frac{\partial P}{\partial I}\right) = \left(\frac{e\lambda}{hc}\right) \Delta\left(\frac{\partial P}{\partial I}\right) \quad (2.13)$$

where  $e$  is the fundamental unit of electric charge,  $h$  is Planck's constant and  $\nu$  is the frequency of light given as  $c/\lambda$ . The quantum efficiency is then found to be  $\eta = 0.495 \pm 0.00021$ . The interpretation of this value is that on an average, for every 2 ( $\sim 1/\eta$ ) electrons injected into the laser diode, 1 photon is emitted.

#### 2.1.5 Calibration of variable attenuator

We observe that controlling the laser fundamental power by varying the diode current is an inefficient method since, the power of the laser does not vary continuously with the injection current. Instead jumps in power and frequency occur when we do this (known as 'mode hops') [1]. Therefore the previous setup is modified by introducing a rotatable  $\lambda/2$  plate and a beam splitter cube (both of which function as two polarizers), in the beam path between the laser diode and the power meter. The injection current

is fixed at its maximum value for this part of the experiment. First, we check that the beam splitter cube is placed such that it transmits the maximum possible power without the  $\lambda/2$  plate. After this is ensured, the  $\lambda/2$  plate is inserted. Moreover, as done before, in order to precisely adjust the heights and positions of the optical elements, an IR card is used to follow the beam path and ensure that the entire transmitted beam falls completely on the power meter. The schematic set up for this part of the experiment is shown in Figure 2.4.

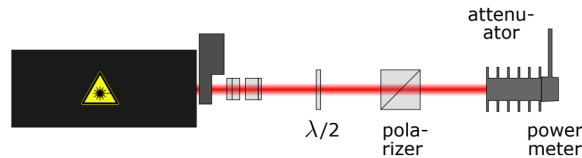


**Figure 2.4:** Schematic set up for variable attenuator calibration [1]

Now, in order to find the dependence of transmitted fundamental power with the angle of polarization, we rotate the  $\lambda/2$  plate in a clockwise direction, starting from  $0^\circ$  upto  $180^\circ$  in increments of  $2.5^\circ$ . A non linear,  $\cos^2 \theta$  form of fitting curve is chosen for this data, since we expected this variation to follow Malus' law. Both the plot of this variation along with the fitting curve are displayed in Figure 2.5.

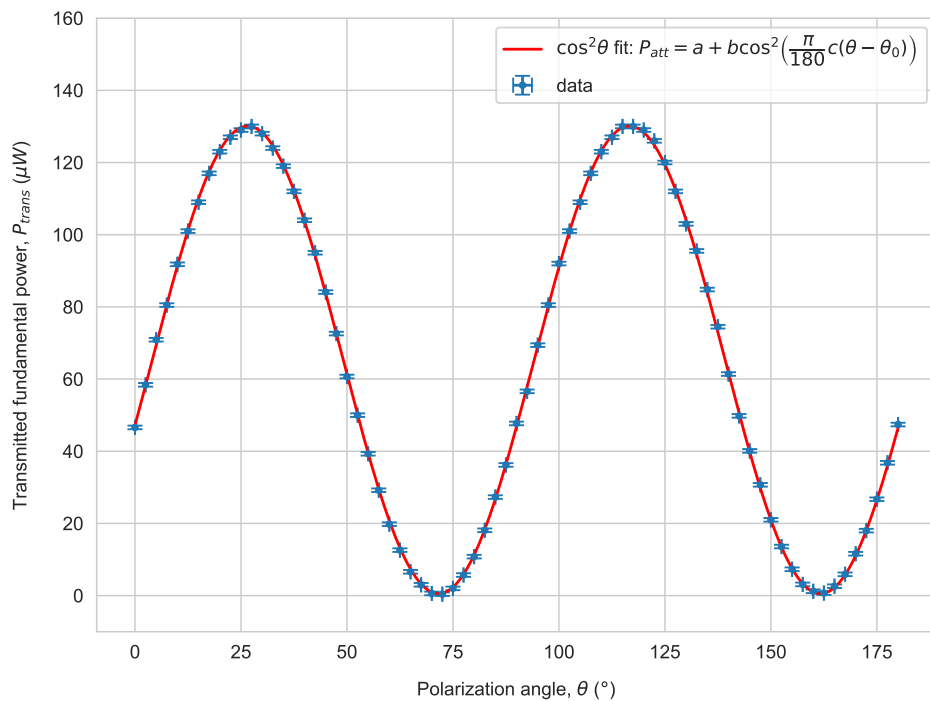


**Figure 2.5:** Plot of the transmitted fundamental power vs the polarization angle of the  $\lambda/2$  plate

# Bibliography

- [1] Universität Bonn, *A245 experiment description*.
- [2] R. Andrae, T. Schulze-Hartung, and P. Melchior, *Dos and don'ts of reduced chi-squared*, 2010.

# Appendix

**Table A.1:** Measured unattenuated and attenuated power of the fundamental beam vs the injection current

$I$ (mA)	$\Delta I$ (mA)	$P_{unatt}$ ( $\mu$ W)	$\Delta P_{unatt}$ ( $\mu$ W)	$P_{att}$ ( $\mu$ W)	$\Delta P_{att}$ ( $\mu$ W)
0	0.5	0	0.01	0	0
5	0.5	1.4	0.01	0	0
10	0.5	3	0.01	0	0
15	0.5	5.1	0.01	0	0
20	0.5	7.3	0.01	0	0
25	0.5	9.6	0.01	0	0
30	0.5	12.2	0.1	0	0
35	0.5	15.6	0.1	0	0
40	0.5	18.6	0.1	0	0
45	0.5	22.7	0.1	0	0
50	0.5	28.2	0.1	0.03	0.01
55	0.5	235	20	0.04	0.01
60	0.5	3130	20	3.2	0.01
65	0.5	5650	20	5.8	0.01
70	0.5	9120	20	8.93	0.01
75	0.5	12900	100	12.6	0.1
80	0.5	16200	100	15.7	0.1
85	0.5	19000	100	18.1	0.1
90	0.5	21730	104	21.6	0.1
95	0.5	25048	106	24.9	0.1
100	0.5	28064	107	27.9	0.1
105	0.5	30879	108	30.7	0.1
110	0.5	33995	109	33.8	0.1
115	0.5	36508	111	36.3	0.1
120	0.5	40630	113	40.4	0.1
125	0.5	43847	115	43.6	0.1
130	0.5	47064	117	46.8	0.1
135	0.5	49778	119	49.5	0.1
140	0.5	53095	121	52.8	0.1
145	0.5	56212	123	55.9	0.1
150	0.5	60132	126	59.8	0.1
155	0.5	63249	128	62.9	0.1
160	0.5	65058	130	64.7	0.1
165	0.5	68476	133	68.1	0.1
170	0.5	71190	135	70.8	0.1
175	0.5	74709	138	74.3	0.1
180	0.5	76820	140	76.4	0.1
185	0.5	80740	143	80.3	0.1
190	0.5	84661	147	84.2	0.1
195	0.5	86470	148	86	0.1
200	0.5	89888	152	89.4	0.1
205	0.5	93608	155	93.1	0.1
210	0.5	99137	160	98.6	0.1
215	0.5	98534	160	98	0.1
Continued on next page					

Table A.1 – continued from previous page

$I$ (mA)	$\Delta I$ (mA)	$P_{unatt}$ ( $\mu$ W)	$\Delta P_{unatt}$ ( $\mu$ W)	$P_{att}$ ( $\mu$ W)	$\Delta P_{att}$ ( $\mu$ W)
220	0.5	100544	162	100	0.1
225	0.5	106576	520	106	0.5
230	0.5	109592	521	109	0.5
235	0.5	109592	521	109	0.5
240	0.5	114618	523	114	0.5
245	0.5	117634	524	117	0.5
250	0.5	120650	525	120	0.5
255	0.5	121655	526	121	0.5
260	0.5	125676	527	125	0.5
265	0.5	132713	530	132	0.5
270	0.5	134724	531	134	0.5
275	0.5	134724	531	134	0.5
280	0.5	141761	533	141	0.5

**Table A.2:** Transmitted fundamental beam power measured at different angles of polarization

$\theta$ ( $^\circ$ )	$\Delta\theta$ ( $^\circ$ )	$P_{trans}$ ( $\mu\text{W}$ )	$\Delta P_{trans}$ ( $\mu\text{W}$ )	$\theta$ ( $^\circ$ )	$\Delta\theta$ ( $^\circ$ )	$P_{trans}$ ( $\mu\text{W}$ )	$\Delta P_{trans}$ ( $\mu\text{W}$ )
0	0.5	46.6	0.5	92.5	1	56.6	0.5
2.5	1	58.4	0.5	95	0.5	69.4	0.5
5	0.5	70.9	0.5	97.5	1	80.5	0.5
7.5	1	80.5	0.5	100	0.5	92	0.5
10	0.5	91.8	0.5	102.5	1	101	0.5
12.5	1	101	0.5	105	0.5	109	0.5
15	0.5	109	0.5	107.5	1	117	0.5
17.5	1	117	0.5	110	0.5	123	0.5
20	0.5	123	0.5	112.5	1	127	0.5
22.5	1	127	0.5	115	0.5	130	0.5
25	0.5	129	0.5	117.5	1	130	0.5
27.5	1	130	0.5	120	0.5	129	0.5
30	0.5	128	0.5	122.5	1	126	0.5
32.5	1	124	0.5	125	0.5	120	0.5
35	0.5	119	0.5	127.5	1	112	0.5
37.5	1	112	0.5	130	0.5	103	0.5
40	0.5	104	0.5	132.5	1	95.5	0.5
42.5	1	95	0.5	135	0.5	84.8	0.5
45	0.5	84.1	0.5	137.5	1	74.5	0.5
47.5	1	72.6	0.5	140	0.5	61.4	0.5
50	0.5	60.7	0.5	142.5	1	49.8	0.5
52.5	1	50	0.5	145	0.5	40.1	0.5
55	0.5	39.3	0.5	147.5	1	30.7	0.5
57.5	1	29.2	0.5	150	0.5	21	0.5
60	0.5	19.8	0.5	152.5	1	13.6	0.5
62.5	1	12.6	0.5	155	0.5	7.3	0.5
65	0.5	6.6	0.5	157.5	1	3.1	0.5
67.5	1	3	0.5	160	0.5	1.2	0.5
70	0.5	0.6	0.5	162.5	1	0.7	0.5
72.5	1	0.4	0.5	165	0.5	2.6	0.5
75	0.5	2	0.5	167.5	1	5.9	0.5
77.5	1	5.7	0.5	170	0.5	11.6	0.5
80	0.5	10.8	0.5	172.5	1	18	0.5
82.5	1	18.1	0.5	175	0.5	26.7	0.5
85	0.5	27.3	0.5	177.5	1	36.8	0.5
87.5	1	36.2	0.5	180	0.5	47.4	0.5
90	0.5	47.7	0.5				